INTERNATIONAL JOURNAL FOR NUMERICAL METHODS IN FLUIDS, VOL. 9, 1099–1111 (1989)

SECOND-ORDER FINITE DIFFERENCE SOLUTIONS FOR THE FLOW BETWEEN ROTATING CONCENTRIC SPHERES

STEVE SCHWENGELS AND DAVID SCHULTZ

University of Wisconsin–Milwaukee, Dept. of Mathematics, Milwaukee, Wisconsin 53201, U.S.A.

AND

WILLIAM SHAY

University of Wisconsin–Green Bay, Dept. of Mathematics, Green Bay, Wisconsin 54311, U.S.A.

SUMMARY

This paper describes a second-order method to calculate approximate solutions to flow of viscous incompressible fluid between rotating concentric spheres. The governing partial differential equations are presented in the stream–vorticity formulation and are written as a series of second-order equations. The technique employed makes use of second-order approximations for all terms in the governing equations and is dependent upon the direction of flow at a given point. This upwind technique has allowed us to generate approximate solutions with larger Reynolds numbers than has generally been possible for second and higher-order techniques. Solutions have been obtained with Reynolds numbers as large as 3000 and with grids as fine as a 40×40 mesh. Results are displayed in the form of level curves for both the stream and vorticity functions. A dimensionless quantity related to the torque acting on both spheres has been calculated from the approximate solution and compared with other results. Results with smaller Reynolds numbers such as 100 and 1000 are in excellent agreement with other published results.

KEY WORDS Navier–Stokes Finite differences Reynolds number Rotating concentric spheres Stream function Second order accuracy Vorticity function

INTRODUCTION

The purpose of this paper is the development of a new approximation technique to calculate the numerical solution of a class of Navier–Stokes problems. The problem under study is that of the flow of a viscous incompressible fluid between two rotating concentric spheres. It is felt that the application of a new numerical technique to the rotating spheres problem is appropriate for two reasons. First, researchers in numerical analysis and fluid dynamics are always interested in numerical techniques that are accurate and stable for a wide range of parameters (see References). As such, the technique under study is of second-order accuracy and when applied to the spheres problem has generated numerical solutions with Reynolds numbers as large as 3000. Secondly, fluid motion inside rotating containers has a variety of applications in engineering such as the study of gyroscopes and centrifuges. Applications also arise in geophysics where atmospheric and oceanic circulations are studied.[1–4] The spherical geometry was chosen partly because of its applications and partly because the Navier–Stokes equations, written in spherical co-ordinates, are a particularly difficult set of partial differential equations to solve and represent a good benchmark for the numerical technique developed.

0271–2091/89/091099–13$06.50

Received January 1988
Revised 22 September 1988

The problem to be studied may be formulated as follows. Consider two concentric spheres centred at the origin with radii r_1 and r_2 respectively (Figure 1). The outer and inner spheres rotate about the y-axis at angular speeds of w_1 and w_2. Thus the fluid contained in the spherical annulus bounded by the spheres is set into motion.

By the assumption of rotational symmetry, it is sufficient to study only a cross-section of the region formed by intersecting the spherical annulus with quadrant I of the x–y plane (Figure 2). Thus if (r, θ) represent the polar co-ordinates in the plane, then the dimensionless Navier–Stokes equations to be satisfied are

$$\mathrm{D}^2\psi = M, \tag{1}$$

$$\mathrm{D}^2\Omega + \frac{Re}{r^2\sin\theta}\left(\frac{\partial\psi}{\partial r}\frac{\partial\Omega}{\partial\theta} - \frac{\partial\psi}{\partial\theta}\frac{\partial\Omega}{\partial r}\right) = 0, \tag{2}$$

$$\mathrm{D}^2 M + Re\left[\frac{2\Omega}{r^3\sin^2\theta}\left(\frac{\partial\Omega}{\partial\theta}\sin\theta - \frac{\partial\Omega}{\partial r}r\cos\theta\right) + \frac{1}{r^2\sin\theta}\left(\frac{\partial\psi}{\partial r}\frac{\partial M}{\partial\theta} - \frac{\partial\psi}{\partial\theta}\frac{\partial M}{\partial r}\right) + \frac{2M}{r^3\sin^2\theta}\left(\frac{\partial\psi}{\partial\theta}\sin\theta - \frac{\partial\psi}{\partial r}r\cos\theta\right)\right] = 0, \tag{3}$$

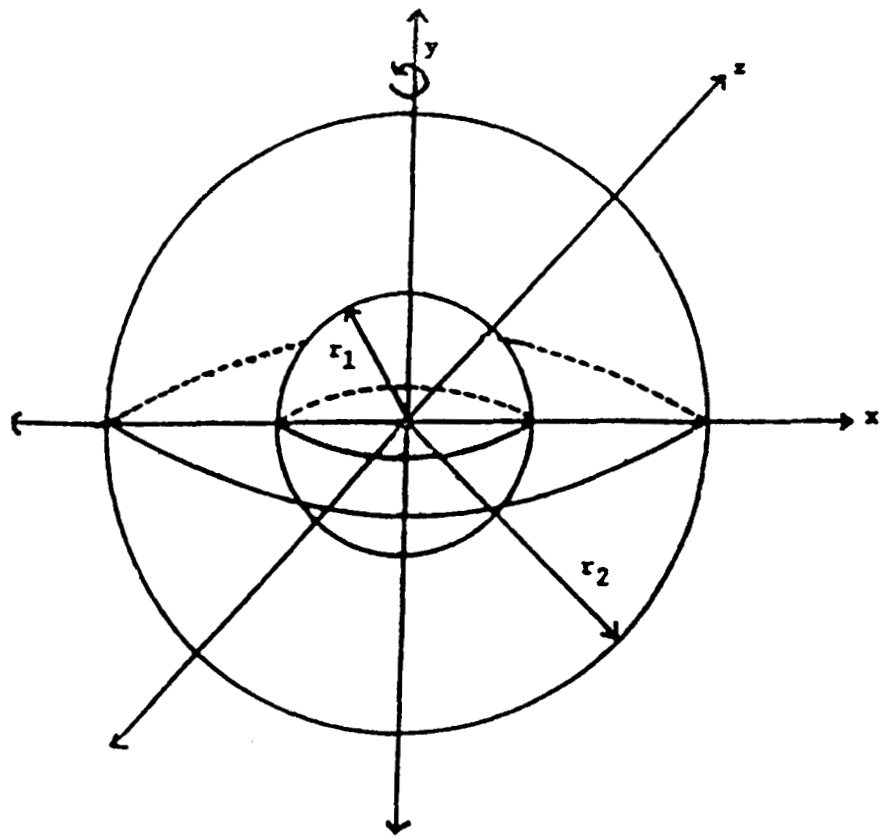

Figure 1

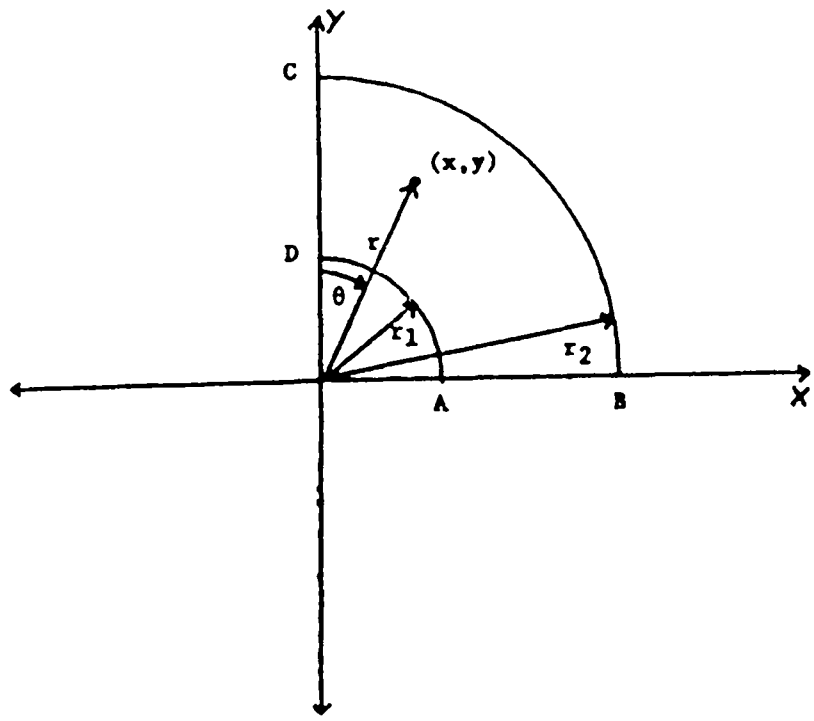

Figure 2

where

$$D^2 = \frac{\partial^2}{\partial r^2} + \frac{1}{r^2}\frac{\partial^2}{\partial \theta^2} - \frac{1}{r^2}\cot\theta\frac{\partial}{\partial \theta}.$$

The velocity vector is given by $\mathbf{V} = (u, v, w)$ where u and v are the velocity components in the direction of increasing r and θ respectively, and w is the component perpendicular to the meridional plane. The streamfunction and vorticity are related to V by

$$u = \frac{\partial \psi}{\partial \theta}/r^2 \sin\theta, \tag{4}$$

$$v = -\frac{\partial \psi}{\partial r}/r \sin\theta, \tag{5}$$

$$w = \Omega/r \sin\theta. \tag{6}$$

The Reynolds number Re is proportional to

$$(w_2 - w_1)^2 (r_2 - r_1)/\nu,$$

where ν is the kinematic viscosity of the fluid. Boundary conditions for this problem may be written as

$$\psi = \partial\psi/\partial r = 0 \quad \text{on arcs AD and BC,} \tag{7}$$

$$\psi = \Omega = M = 0 \quad \text{on CD,} \tag{8}$$

$$\Omega = w_1 r_1^2 \sin^2\theta \quad \text{on AD,} \tag{9}$$

$$\Omega = w_2 r_2^2 \sin^2\theta \quad \text{on BC.} \tag{10}$$

The numerical technique to be applied to the above problem is a finite difference technique. However, what is of particular interest is that different approximations to the spatial derivatives are made at different grid points. In other words, before generating discrete approximations to equations (2)–(3) at a specific point, the direction of the flow at the point is examined. This is easily done by checking the signs of ψ_r and ψ_θ.

Next a finite difference approximation dependent on these values is generated which constitutes one of many equations in the unknown values for ψ, Ω and M obtained through similar expansion at all the other grid points. Through appropriate selection of finite differences, a system of equations is generated whose matrix of coefficients does not contain diagonal elements whose magnitudes become arbitrarily small with respect to the magnitudes of the off-diagonal elements. As a result, iterative techniques such as successive over-relaxation used to approximate solutions to systems of equations may be more successfully applied to the generated system of equations. This technique is similar to that employed by Greenspan[5] and Schultz and Greenspan[6] in an application of the upwind finite difference technique to the problem of fluid inside rotating spheres. However, what makes the current technique attractive is that all approximations are chosen to be second-order accurate.

Dennis and Quartapelle[7] present solutions to this problem for large grid sizes and for Reynolds numbers up to 1000. Dennis and Singh,[8] using the method of series truncation, obtained solutions for Reynolds numbers up to 2000. Stewartson[4] and Pedlosky[3] and others used singular perturbation techniques. Pearson[9] obtained solutions for Reynolds numbers from 10 to 1500. Munson and Joseph[10] used a perturbation method for small Reynolds numbers and a series representation technique to obtain solutions for Reynolds numbers up to 1000. Also some experimental work was done on this problem by Wimmer.[11]

The technique described in this paper has been successfully applied to this problem for values of the Reynolds number as large as 3000 and for grids containing as many as 40 points in both the directions of r and θ. Results are given for the stream and vorticity functions for a range of Reynolds numbers and grids. In addition, a dimensionless coefficient related to torque on the spheres is numerically computed from approximate solutions produced by the technique. Displays of the data are made as a function of Re and mesh size and results are compared with those in other works.

METHOD

To implement the finite difference technique, an array of nodes is placed over the region in Figure 2. The distance between two consecutive points along the arc r = constant is given by $\Delta\theta$, and the distance between two consecutive points along the line θ = constant is given by Δr. Next, finite difference approximations to equations (1), (2) and (3) are generated at each node inside the region as follows.

An approximation to $D^2\psi = \psi_{rr} + (1/r^2)\psi_{\theta\theta} - (1/r^2)(\cot\theta)\psi_\theta = M$ may be written as (see Figure 3)

$$\frac{\psi_1 - 2\psi_0 + \psi_3}{\Delta r^2} + \frac{\psi_2 - 2\psi_0 + \psi_4}{r^2\Delta\theta^2} - \frac{(\psi_2 - \psi_4)\cot\theta}{2r^2\Delta\theta}$$

$$= \left(\frac{-2}{\Delta r^2} - \frac{2}{r^2\Delta\theta^2}\right)\psi_0 + \left(\frac{1}{\Delta r^2}\right)\psi_1 + \left(\frac{1}{r^2\Delta\theta^2} - \frac{\cot\theta}{2r^2\Delta\theta}\right)\psi_2$$

$$+ \left(\frac{1}{\Delta r^2}\right)\psi_3 + \left(\frac{1}{r^2\Delta\theta^2} + \frac{\cot\theta}{2r^2\Delta\theta}\right)\psi_4 = M. \tag{11}$$

The truncation error in the approximation of each term is $O(\Delta r^2)$ or $O(\Delta\theta^2)$.

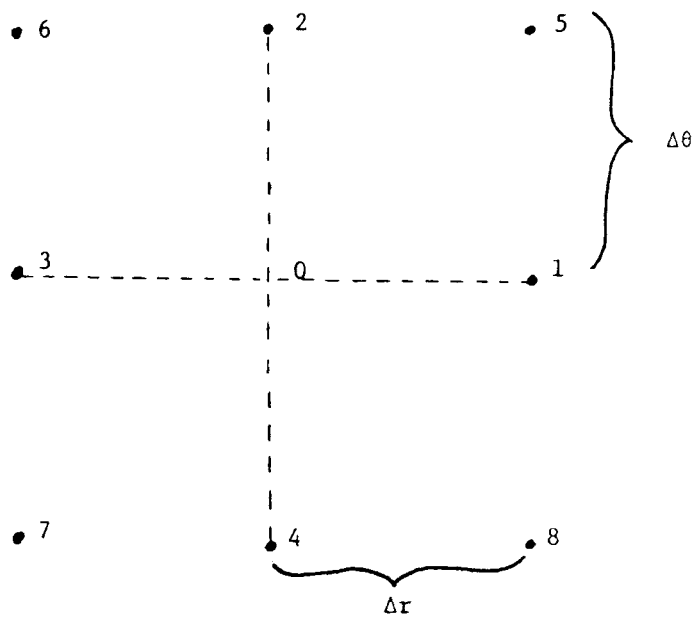

Figure 3

When equation (11) is applied at each point inside the region, the result is a system of equations, linear in unknown ψ values, whose matrix of coefficients has the property that the magnitude of the diagonal element is greater than or equal to the sum of the magnitudes of the off-diagonal elements within any row.

Multiplication of both sides of equation (11) by Δr^2 yields

$$\left(-2-\frac{2\varepsilon^2}{r^2}\right)\psi_0+\psi_1+\left(\frac{\varepsilon^2}{r^2}-\frac{\varepsilon\Delta r\cot\theta}{2r^2}\right)\psi_2+\psi_3+\left(\frac{\varepsilon^2}{r^2}+\frac{\varepsilon\Delta r\cot\theta}{2r^2}\right)\psi_4=\Delta r^2 M, \tag{12}$$

where $\varepsilon=\Delta r/\Delta\theta$. Similar approximations are made for D^2M and $\mathrm{D}^2\Omega$.

In order to generate an approximation for the term $(Re/r^2\sin\theta)[\psi_r\Omega_\theta-\psi_\theta\Omega_r]$ in equation (2), write

$$\frac{Re}{r^2\sin\theta}[\psi_r\Omega_\theta-\psi_\theta\Omega_r]=\sum_{i=0}^{8}\alpha_i\Omega_i. \tag{13}$$

The α_i will be chosen so that $\sum_{i=0}^{8}\alpha_i\Omega_i$ represents a second-order approximation to $(Re/r^2\sin\theta)[\psi_r\Omega_\theta-\psi_\theta\Omega_r]$. Furthermore, the direction of flow partly determines the choices of the α_i, so that the magnitude of the diagonal elements in the final coefficient matrix remain large relative to the magnitudes of the off-diagonal elements. This technique gives a very stable system which allows one to obtain solutions for larger Reynolds numbers than has generally been possible for high-order methods. Next, expand each of the Ω_i above in a Taylor series about the central point in Figure 3 up through third-order terms and then combine terms with like

derivatives. This yields

$$\begin{aligned}\frac{Re}{r^2\sin\theta}[\psi_r\Omega_\theta-\psi_\theta\Omega_t]=&\left(\sum_{i=0}^{8}\alpha_i\right)\Omega_0+\Delta r(\alpha_1-\alpha_3+\alpha_5-\alpha_6-\alpha_7+\alpha_8)\Omega_r\\&+\Delta\theta(\alpha_2-\alpha_4+\alpha_5+\alpha_6-\alpha_7-\alpha_8)\Omega_\theta\\&+\left(\frac{\Delta r^2}{2}\right)(\alpha_1+\alpha_3+\alpha_5+\alpha_6+\alpha_7+\alpha_8)\Omega_{rr}\\&+\Delta r\Delta\theta(\alpha_5-\alpha_6+\alpha_7-\alpha_8)\Omega_{r\theta}\\&+\left(\frac{\Delta\theta^2}{2}\right)(\alpha_2+\alpha_4+\alpha_5+\alpha_6+\alpha_7+\alpha_8)\Omega_{\theta\theta}\\&+\left(\frac{\Delta r^3}{6}\right)(\alpha_1-\alpha_3+\alpha_5-\alpha_6-\alpha_7+\alpha_8)\Omega_{rrr}\\&+\left(\frac{\Delta r^2\Delta\theta}{2}\right)(\alpha_5+\alpha_6-\alpha_7-\alpha_8)\Omega_{rr\theta}\\&+\left(\frac{\Delta r\Delta\theta^2}{2}\right)(\alpha_5-\alpha_6-\alpha_7+\alpha_8)\Omega_{r\theta\theta}\\&+\left(\frac{\Delta\theta^3}{6}\right)(\alpha_2-\alpha_4+\alpha_5+\alpha_6-\alpha_7-\alpha_8)\Omega_{\theta\theta\theta}.\end{aligned}\tag{14}$$

The error term is $O(\Delta r^4+\Delta\theta^4)$.

By equating coefficients of like terms of Ω and its partial derivatives, we get

$$\sum_{i=0}^{8}\alpha_i=0,\tag{15}$$

$$\alpha_1-\alpha_3+\alpha_5-\alpha_6-\alpha_7+\alpha_8=-Re\psi_\theta/r^2\Delta r\sin\theta,\tag{16}$$

$$\alpha_2-\alpha_4+\alpha_5+\alpha_6-\alpha_7-\alpha_8=Re\psi_r/r^2\Delta\theta\sin\theta,\tag{17}$$

$$\alpha_1+\alpha_3+\alpha_5+\alpha_6+\alpha_7+\alpha_8=0,\tag{18}$$

$$\alpha_5-\alpha_6+\alpha_7-\alpha_8=0,\tag{19}$$

$$\alpha_2+\alpha_4+\alpha_5+\alpha_6+\alpha_7+\alpha_8=0.\tag{20}$$

The first equation results from equating coefficients of Ω_0, the next two result from equating coefficients of the first partial derivatives of Ω, and the next three result from equating coefficients of the second partials of Ω. Any attempt to equate coefficients of the third partial derivatives of Ω (specifically Ω_{rrr} and $\Omega_{\theta\theta\theta}$) results in equating the linear combinations of the α_i that appear in (16) and (17) above to 0. This results in an inconsistent system of equations. Thus the inability to equate coefficients of these third partial derivatives results in error terms proportional $(\Delta r)^3$ and $(\Delta\theta)^3$. Since Δr and $\Delta\theta$ are of the same order of magnitude, there is no need to attempt to equate coefficients of $\Omega_{r\theta\theta}$ and $\Omega_{rr\theta}$. Thus additional error terms proportional to $\Delta r(\Delta\theta)^2$ and $(\Delta r)^2\Delta\theta$ will be generated. However, these will be of the same order as the unavoidable error terms. The advantages are fewer constraints on the α_i and a greater flexibility in choosing an approximation based on the flow at any point.

Treating α_6, α_7 and α_8 as independent choices, equations (15)–(20) imply

$$\alpha_0 = 2(\alpha_6 + \alpha_8), \tag{21}$$

$$\alpha_1 = -\frac{Re\psi_\theta}{2r^2\Delta r \sin\theta} - \alpha_6 + \alpha_7 - 2\alpha_8, \tag{22}$$

$$\alpha_2 = \frac{Re\psi_r}{2r^2\Delta\theta \sin\theta} - 2\alpha_6 + \alpha_7 - \alpha_8, \tag{23}$$

$$\alpha_3 = \frac{Re\psi_\theta}{2r^2\Delta r \sin\theta} - \alpha_6 - \alpha_7, \tag{24}$$

$$\alpha_4 = -\frac{Re\psi_r}{2r^2\Delta\theta \sin\theta} - \alpha_7 - \alpha_8, \tag{25}$$

$$\alpha_5 = \alpha_6 - \alpha_7 + \alpha_8. \tag{26}$$

Since the direction of flow is represented by the signs of ψ_r and ψ_θ, the choices of α_6, α_7 and α_8 are as described in Table I. In each case it can be shown that

$$\alpha_0 = -\frac{Re}{r^2 \sin\theta}\left(\frac{|\psi_r|}{\Delta\theta} + \frac{|\psi_\theta|}{\Delta r}\right), \tag{27}$$

$$\alpha_1 = \alpha_2 = \alpha_3 = \alpha_4 = \frac{Re}{2r^2 \sin\theta}\left(\frac{|\psi_r|}{\Delta\theta} + \frac{|\psi_\theta|}{\Delta r}\right), \tag{28}$$

$$\alpha_5 = -\frac{Re}{2r^2 \sin\theta}\left(\frac{|\psi_\theta| + \psi_\theta}{2\Delta r} + \frac{|\psi_r| - \psi_r}{2\Delta\theta}\right). \tag{29}$$

Unfortunately this will not yield a diagonally dominant matrix of coefficients, but on the other hand it is easily shown that

$$\sum_{i=1}^{8} |\alpha_i| \leqslant 3|\alpha_0|.$$

Furthermore, since α_0 is guaranteed to be negative, when equation (13) is combined with the approximation for $D^2\Omega$ described previously, the ratio of the sum of the magnitudes of the off-

Table I. Definitions of α_6, α_7 and α_8 as functions of the signs of ψ_r and ψ_θ

	α_6	α_7	α_8
$\psi_r \geqslant 0, \psi_\theta \geqslant 0$	0	$-\frac{Re\psi_r}{2r^2\Delta\theta \sin\theta}$	$-\frac{Re}{2r^2 \sin\theta}\left(\frac{\psi_r}{\Delta\theta} + \frac{\psi_\theta}{\Delta r}\right)$
$\psi_r < 0, \psi_\theta \geqslant 0$	$\frac{Re\psi_r}{2r^2\Delta\theta \sin\theta}$	0	$-\frac{Re\psi_\theta}{2r^2\Delta r \sin\theta}$
$\psi_r \geqslant 0, \psi_\theta < 0$	$\frac{Re\psi_\theta}{2r^2\Delta r \sin\theta}$	$\frac{Re}{2r^2 \sin\theta}\left(\frac{\psi_\theta}{\Delta r} - \frac{\psi_r}{\Delta\theta}\right)$	$-\frac{Re\psi_r}{2r^2\Delta\theta \sin\theta}$
$\psi_r < 0, \psi_\theta < 0$	$\frac{Re}{2r^2 \sin\theta}\left(\frac{\psi_r}{\Delta\theta} + \frac{\psi_\theta}{\Delta r}\right)$	$\frac{Re\psi_\theta}{2r^2\Delta r \sin\theta}$	0

diagonal terms to the magnitude of the diagonal term in the coefficient matrix is bounded by a constant independent of Re. If central difference approximations are used for ψ_r and ψ_θ, then the discretization of equation (2) is complete.

In order to generate an approximation for equation (3), the terms

$$D^2 M + \frac{1}{r^2 \sin\theta}[\psi_r M_\theta - \psi_\theta M_r]$$

may be approximated by following the same procedure applied to equation (2). The remaining differential terms in equation (3) are all approximated by central difference approximations.

The boundary conditions are handled in a similar way to the methods described in References 5, 6 and 12, with the exception that all boundary conditions used in this paper are second-order. On the line $\theta = \pi/2$ we apply the difference equations with the following symmetry substitution:[5,6]

$$\psi(r, \pi/2 + \Delta\theta) = -\psi(r, \pi/2 - \Delta\theta),$$
$$\Omega(r, \pi/2 + \Delta\theta) = \Omega(r, \pi/2 - \Delta\theta),$$
$$M(r, \pi/2 + \Delta\theta) = -M(r, \pi/2 - \Delta\theta).$$

At each point of AD apply the equation

$$M(r_1, j\Delta\theta) = \frac{3\psi(r_1 + \Delta r, j\Delta\theta)}{\Delta r^2} - \frac{M(r_1 + \Delta r, j\Delta\theta)}{2} \quad \text{for } j = 0, 1, 2, \ldots, \left(\frac{\pi/2}{\Delta\theta}\right). \tag{30}$$

At each point of BC apply the equation

$$M(r_2, j\Delta\theta) = \frac{3\psi(r_2 - \Delta r, j\Delta\theta)}{\Delta r^2} - \frac{M(r_2 - \Delta r, j\Delta\theta)}{2} \quad \text{for } j = 0, 1, 2, \ldots, \left(\frac{\pi/2}{\Delta\theta}\right). \tag{31}$$

See Reference 12 for a development of this type of boundary condition. Now define the inner boundary as the set of grid points that lie a distance Δr from the sides AD and BC. Values at these grid points are used to guarantee that the normal derivative conditions of the streamfunction are satisfied.

Stream values on the inner boundary of the side AD are determined from

$$\psi_{r_0} = (-11\psi_0 + 18\psi_1 - 9\psi_2 + 2\psi_3)/6\Delta r + O(\Delta r^3),$$

where the points are as in Figure 4 and $\psi_{r_0} = \partial\psi/\partial r|_0$. Since $\psi_{r_0} = 0$ and $\psi_0 = 0$, we can solve for ψ_1:

$$\psi_1 = \psi_2/2 - \psi_3/9 + O(\Delta r^4). \tag{32}$$

The higher-order approximation in (32) is used so that when (32) is inserted in (30) the $O(\Delta r^2)$ accuracy is maintained. The formulae for the side BC are similar.

RESULTS AND DISCUSSION

The systems of equations generated by the approximations described in the previous section have been solved by the method of successive over-relaxation. Solutions were obtained for a variety of Reynolds numbers and mesh sizes, including a solution for the case $Re = 3000$ and a 40×40 grid. All results described in this paper were obtained with values of $r_1 = 0{\cdot}5$, $r_2 = 1{\cdot}0$ and either $w_1 = 0$, $w_2 = 1$ or $w_1 = 1$, $w_2 = 0$. (However, a wide variety of cases were run.) The convergence criteria were varied for different Reynolds numbers and mesh sizes, but in all cases the convergence

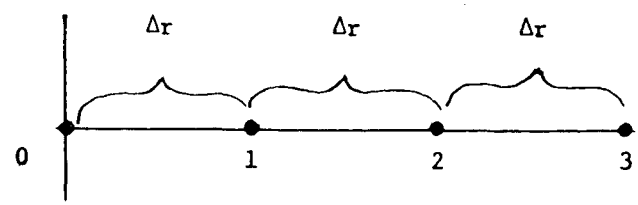

Figure 4

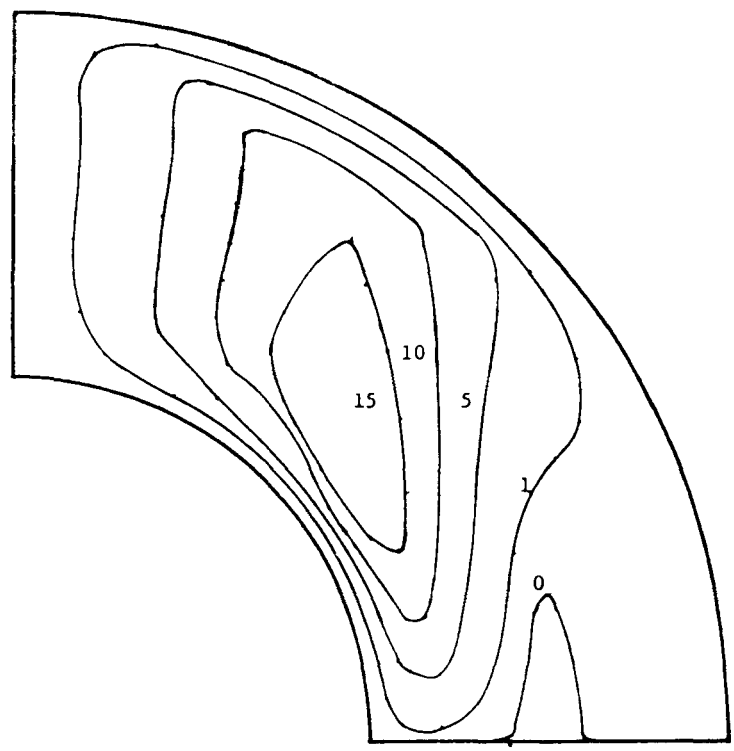

Figure 5. Level ψ curves multiplied by 10^4; $Re = 1000$, $w_1 = 0$, $w_2 = 1$, $\Delta r = 0{\cdot}025$, $\Delta\theta = 2{\cdot}25°$

criterion was below 10^{-5}. Level curves for both ψ and Ω are given in Figures 5–8. Figures 5 and 6 display results for a Reynolds number of 1000 and Figures 7 and 8 display results for a Reynolds number of 3000. Both sets of results correspond to the finest grids attempted for the problems. For $Re = 3000$, mesh sizes are $\Delta r = 0{\cdot}0125$ and $\Delta\theta = 0{\cdot}039$, and for $Re = 1000$, $\Delta r = 0{\cdot}025$ and $\Delta\theta = 0{\cdot}039$.

For small values of the Reynolds number the method converged rapidly, with relaxation parameters of $r_\psi = 1{\cdot}0$, $r_\Omega = 0{\cdot}9$ and $r_M = 0{\cdot}9$. For large Re the method required a small value of r_M for convergence. We would start with a small value of $r_M = 0{\cdot}001$ and slowly increase it until $r_M = 0{\cdot}2$ or $0{\cdot}3$. The accuracy of the results has been checked in several ways. First, comparisons were made between results for $Re = 1000$ displayed in Figures 5 and 6 and those obtained in other works.[5–7,9] These results show the same type of patterns in level curves for ψ and Ω that we observed. All exhibit the existence of a recirculating zone near the equator and disjoint closed

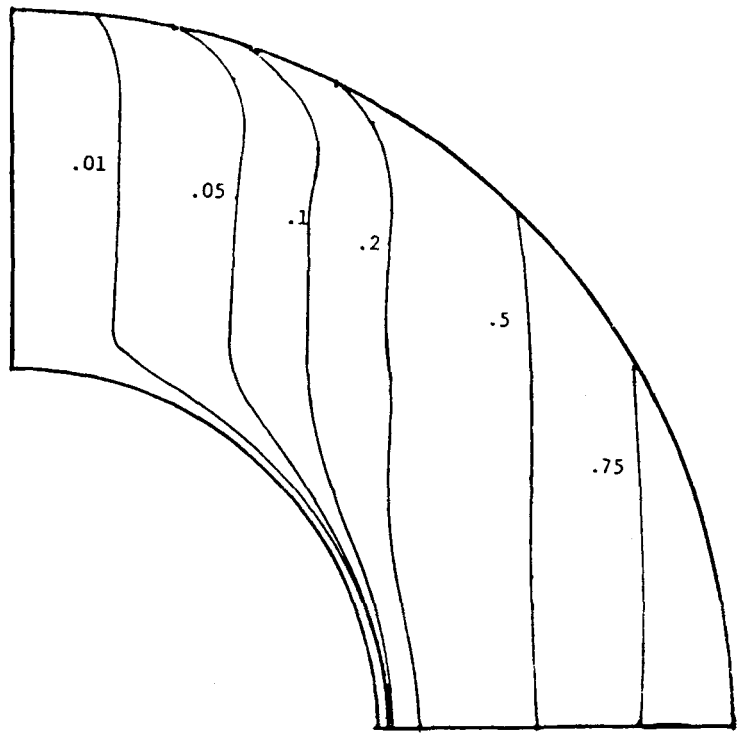

Figure 6. Level Ω curves; $Re = 1000$, $w_1 = 0$, $w_2 = 1$, $\Delta r = 0{\cdot}025$, $\Delta\theta = 2{\cdot}25°$

Table II. Results showing ψ and Ω at $(r, \theta) = (0{\cdot}75, \pi/4)$ with Reynolds number 3000, $w_1 = 0$ and $w_2 = 1$

$(\Delta r, \Delta\theta)$	ψ (at $r = 0{\cdot}75$, $\theta = \pi/4$)	% change	Ω (at $r = 0{\cdot}75$, $\theta = \pi/4$)	% change
(0·05, 0·079)	0·0006132		0·2119	
		18·3%		0·85%
(0·025, 0·039)	0·000725		0·2137	
		2·2%		0·66%
(0·0125, 0·039)	0·0007414		0·2123	

curves for the streamfunction. Another accuracy check was an evaluation of the fully discretized approximations to equations (1) and (2) at the final solution. The results, called residuals, were printed. When the ψ-values from Figure 7 were put into equation (12), the magnitudes of the residuals were bounded above by 10^{-9}; similarly, when the Ω-values from Figure 8 were put into appropriate approximating equations, the magnitudes of the residuals were bounded above by 10^{-7}. A third accuracy check was via a display of solutions written as a function of $\Delta\theta$ and Δr. For example, Table II shows results for ψ and Ω obtained at the midpoint of the region as a function of Δr and $\Delta\theta$. With the last grid refinement, the centre values for ψ changed by only 2·2% and the centre values for Ω changed by less than 1%.

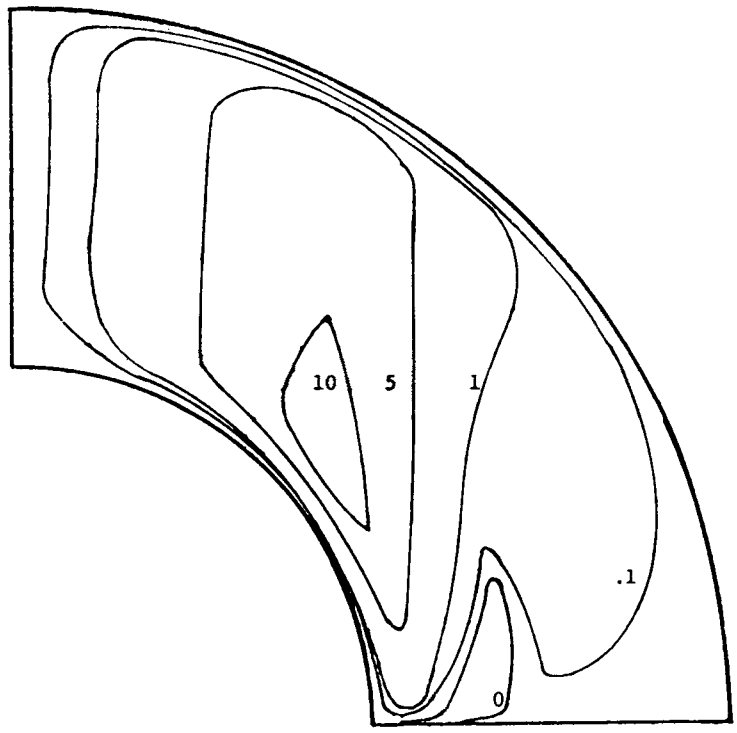

Figure 7. Level ψ curves multiplied by 10^4; $Re = 3000$, $w_1 = 0$, $w_2 = 1$, $\Delta r = 0{\cdot}0125$, $\Delta\theta = 2{\cdot}25°$

A final check for accuracy was made through the calculation of a dimensionless coefficient related to the torque, defined in Reference 8 by

$$C = \frac{3}{2}\int_0^{\pi/2} r^3\left(\frac{\partial w}{\partial r} - \frac{w}{r}\right)\sin^2\theta \, d\theta.$$

Through the use of equation (6), this becomes

$$C = \frac{3}{2}\int_0^{\pi/2} r\sin\theta\left(r\frac{\partial\Omega}{\partial r} - 2\Omega\right)d\theta.$$

The integral is to be evaluated on either sphere. When evaluated on both spheres, the integral should yield values that are opposites.

Table III depicts the approximated integral values for a range of solutions. The integral was evaluated using Simpson's rule and second-order accurate, three-point approximation for $\partial\Omega/\partial r$. Results in Table III are comparable with corresponding results recently published in Reference 7. In fact, because of a more refined grid and strict convergence criterion, we show better agreement between the non-dimensional torque on both spheres for $Re = 1000$.

CONCLUSIONS

This work has shown that the described method is capable of producing accurate results not generally obtainable for large values of Re. Results obtained for $Re = 100$ and 1000 are in good

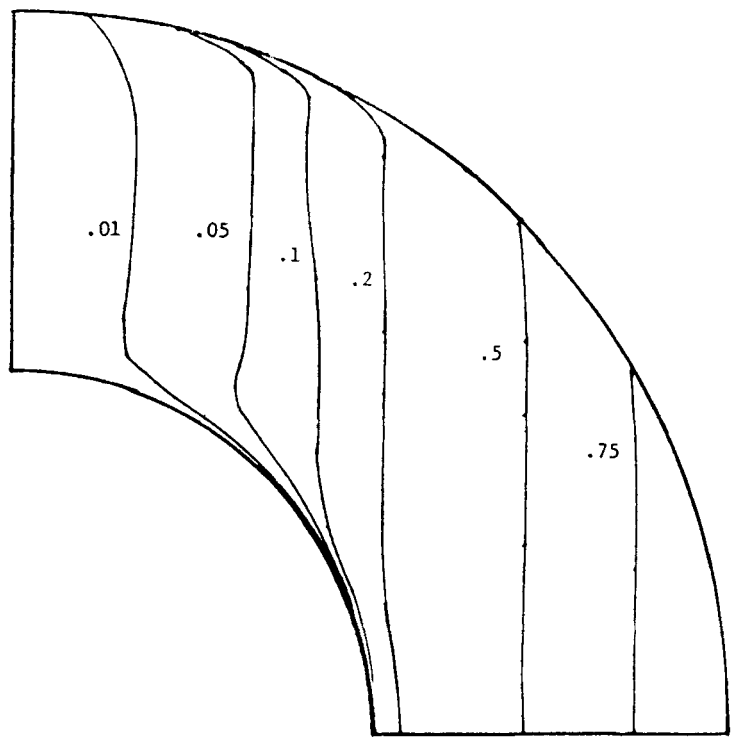

Figure 8. Level Ω curves; $Re = 3000$, $w_1 = 0$, $w_2 = 1$, $\Delta r = 0{\cdot}0125$, $\Delta\theta = 2{\cdot}25°$

Table III. Results showing $|\frac{3}{2}\int_0^{\pi/2} r\sin\theta\,(r\partial\Omega/\partial r - 2\Omega)\,d\theta|$ on the inner and outer spheres. For $Re = 100$ we used $w_1 = 1$ and $w_2 = 0$, and for $Re = 1000$ and 3000 we used $w_1 = 0$ and $w_2 = 1$

Re	$(\Delta r, \Delta\theta)$	$\lvert C\rvert$ on inner sphere	$\lvert C\rvert$ on outer sphere	% difference
100	(0·1, 0·157)	0·4326	0·4500	3·9%
100	(0·05, 0·079)	0·4451	0·4479	0·6%
100	(0·025, 0·039)	0·4465	0·4464	0·02%
1000	(0·05, 0·079)	0·9391	0·8907	5·2%
1000	(0·025, 0·039)	0·9043	0·9201	1·7%
3000	(0·05, 0·079)	1·1813	1·0491	11·2%
3000	(0·025, 0·039)	1·3382	1·2963	3·1%
3000	(0·0125, 0·039)	1·2567	1·3004	3·4%

agreement with other published results. Furthermore, the accuracy checks imposed on the approximated solution indicate a reasonably high level of accuracy for a Reynolds number of 3000. These facts suggest that the method is a powerful and accurate one suitable for a difficult set of partial differential equations.

REFERENCES

1. H. P. Greenspan, *The Theory of Rotating Fluids*, Cambridge University Press, 1968.
2. C. E. Pearson, *Studies in Numerical Analysis, Vol. 1*, SIAM, Philadelphia, 1969, p. 65.
3. J. Pedlosky, 'Axially symmetric motion of a stratified, rotating fluid in a spherical annulus of narrow gap', *J. Fluid Mech.*, **36**, 401 (1969).
4. K. Stewartson, 'On almost rigid motions', *J. Fluid Mech.*, **26**, 131 (1966).
5. D. Greenspan, 'Numerical studies of steady, viscous, incompressible flow between two rotating spheres', *Comput. Fluids*, **3**, 69 (1975).
6. D. Schultz and D. Greenspan, 'Improved solution of steady, viscous, incompressible flow between two rotating spheres', *Comput. Fluids*, **7**, 157 (1979).
7. S. C. R. Dennis and L. Quartapelle, 'Finite difference solution to the flow between two rotating spheres', *Comput. Fluids*, **12**, 77 (1984).
8. S. C. R. Dennis and S. N. Singh, 'Calculation of the flow between two rotating spheres by the method of series truncation', *J. Comput. Phys.*, **28**, 297 (1978).
9. C. E. Pearson, 'A numerical study of time dependent viscous flow between two rotating spheres', *J. Fluid Mech.*, **28**, 323 (1967).
10. B. R. Munson and D. D. Joseph, 'Viscous incompressible flow between concentric rotating spheres, Part 1. Basic flow', *J. Fluid Mech.*, **49**, 289 (1971).
11. M. Wimmer, 'Experiments on a viscous fluid flow between concentric rotating spheres', *J. Fluid Mech.*, **78**, 317 (1976).
12. A. K. Runchal, D. B. Spalding and M. Wolfshtein, 'The numerical solution of the elliptic equations for transport of vorticity, heat and matter in two dimensional flows', *Ref. No. SF/TN/14*, Department of Mechanical Engineering, Imperial College, London, 1968.